Theor Chem Acc (2005) 113: 95–106
DOI 10.1007/s00214-004-0612-1

Theoretical
Chemistry Accounts

*Regular Article*

# Symmetry or asymmetry in cheletropic additions forming cyclopropanes

**Shinichi Yamabe**[1], **Noriko Tsuchida**[1], **Tsutomu Minato**[2], **Takahisa Machiguchi**[3]

[1] Department of Chemistry, Nara University of Education, Takabatake-cho, 630-8528, Nara, Japan
[2] Institute for Natural Science, Nara University, 1500 Misasagi-cho, 631-8502, Nara, Japan
[3] Department of Chemistry, Faculty of Science, Saitama University, 338-8570, Saitama, Japan

Received: 19 March 2004 / Accepted: 11 August 2004 / Published online: 21 February 2005


**Abstract.** Cheletropic additions forming cyclopropane rings were studied theoretically. Ten addition paths were traced by means of density-functional-theory calculations. Two 1,4-dienes, 1,4-pentadiene, and tricyclo[5.3.1.$0^{4,9}$]undeca-2,5-diene were adopted as substrates. CO, $SO_2$, $C_2H_5PCl_2$, $CCl_2$ and $SiCl_2$ were employed as cheletropic reagents (*X*s). An orbital correlation diagram of the Woodward–Hoffmann (W–H) rule and frontier molecular orbital (FMO) interactions between them were investigated in detail. The FMO interactions, HOMO (1,4-diene) → lumo (*X*) and homo (*X*) → LUMO (diene), work reasonably for the progress of the reactions. Those cause the formation of two C–*X* bonds and a cyclopropane ring, and alternation of double bonds to single bonds. All the additions are concerted. The easiness of the ring formation depends upon the energy gap between HOMO and lumo and that between homo and LUMO, and the spatial directions of HOMO and LUMO extensions. Symmetry conservation of the W–H rule does not hold necessarily for those addition paths. The symmetry-breaking was discussed in terms of FMO interactions.

**Keywords:** Cheletropic additions – Frontier molecular orbital – Woodward–Hoffmann rule – Cyclopropane ring – Rehybridization

## 1 Introduction

The present work deals with the cyclopropane-ring formation by cheletropic reactions. The possibility of the ring formation is investigated theoretically. Cheletropic reactions were defined for the first time by Woodward and Hoffmann (W-H) [1]. In those reactions, two $\sigma$ bonds are formed or broken at a single atom. A representative addition reaction is cyclopropanation between olefins and carbenes, Eq. (1).

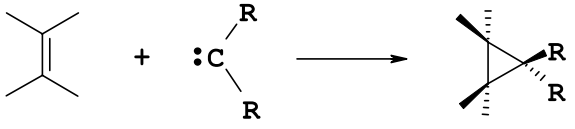


(1)

A typical elimination reaction is the decarbonylation affording a conjugated system in Eq. (2) [2].

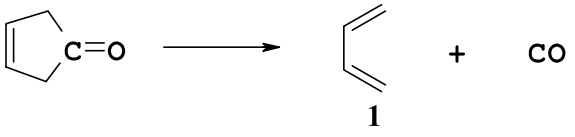


(2)

Cheletropic additions compete with Diels-Alder reactions between dienes and $SO_2$ in Eq. (3) [3].

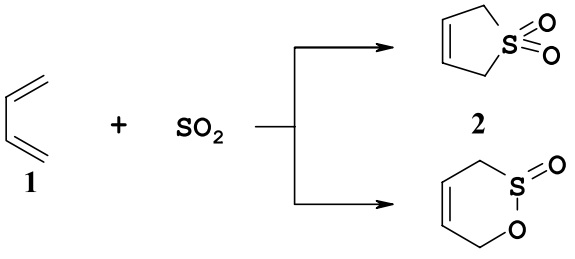


(3)

A dissociative cheletropic reaction involving the cyclopropane-ring opening is shown in Eq. (4) [4].

*Corresponding author*: ShinichiYamabe
e-mail: yamabes@nara-edu.ac.jp

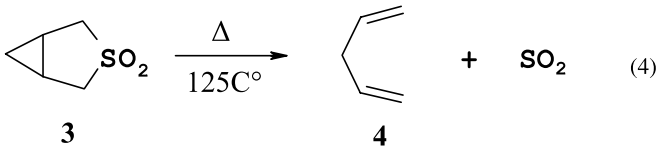

(4)

While there are experimental and theoretical data of those cheletropic reactions, the mechanism of the reactions in Eq. (5) has not been investigated so far.

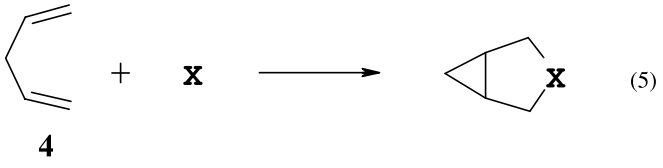

(5)

Although such cyclopropane-ring openings as in Eq. (4) are likely to occur, the reverse ring formation in Eq. (5) would usually be difficult owing to the ring strain.

The novel cheletropic reaction in Eq. (6) was shown to proceed readily [5].

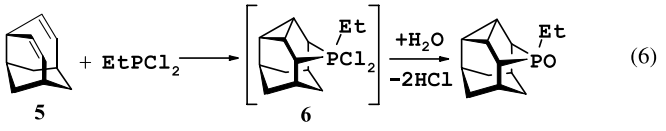

(6)

The reactant, tricyclo[5.3.1.$0^{4,9}$]undeca-2,5-diene (**5**), has the structure of the parent homodiene, penta-1,4-diene (**4**), supported by three axial C–C bonds to a cyclohexyl ring. The reaction takes place in a mild conditions (no solvent, room temperature, 1 day, 70% yield) and is regarded as a new class of the cheletropic reaction [5].

It is tempting to examine whether the new class of the cheletropic reaction is general or not. The driving force of the cyclopropane-ring closure needs to be elucidated in terms of orbital interactions. In this work, we focused our attention on paths of the cheletropic additions, and Eq. (5) was investigated theoretically by the use of the two 1,4-dienes and the five reagents in Scheme 1. The diene **5** is thought to be suitable for the present reactions, because the two double bonds are fixed to be *cis*.

In this work, an orbital correlation diagram of the W–H rule was depicted and indicated that the addition is symmetry-allowed. At the same time, frontier molecular orbital (FMO) [6] interactions between **4** and $SO_2$ were examined. In order to assess predictions of the W–H rule and FMO theory, ten addition paths were determined by the density-functional-theory method. Although the W–H rule predicts the $C_s$-symmetry conserving paths, some combinations in Scheme 1 gave symmetry-breaking ones. The FMO theory was found to be comprehensive for symmetry-conserving and symmetry-breaking paths with clear orbital pictures.

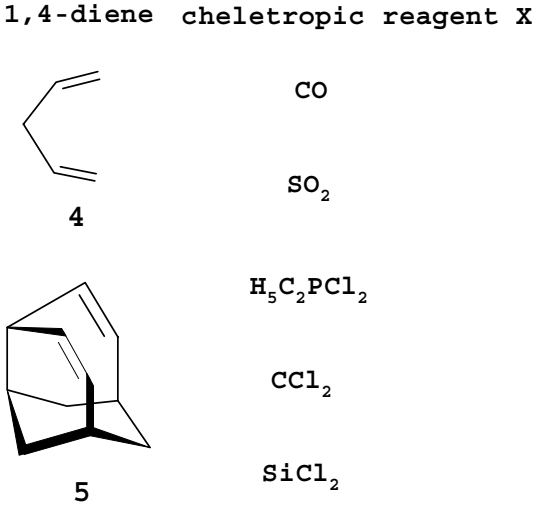


**Scheme 1** Combination of five 1,4-dienes and three cheletropic reagents (*X*s).

## 2 W–H rule and FMO predictions of cheletropic additions involving cyclopropanation

The reaction path of Eq. (5) is predicted in terms of the W–H rule [1] and FMO theory [6] in this section. As an example, a pair of **4** and $SO_2$ was taken up. Figure 1 exhibits occupied and vacant orbitals which are components of an orbital correlation diagram. The W–H rule states that the $C_s$-symmetry conserving cheletropic addition path is symmetry-allowed when the symmetry assignment to the occupied orbitals is the same. In both reactants and adduct, it is (A, S, S) and accordingly the $C_s$-symmetry path is allowed. Figure 1 shows a prediction of the W–H rule. Next, an FMO prediction is explained. The FMOs of **4**, HOMO and LUMO, are shown in Fig. 2 and their nodal properties and spatial extensions are the same as those of *cis*-1,3-butadiene (**1**). HOMO is antisymmetric and LUMO is symmetric with respect to the $C_s$ mirror plane (*m*). The FMOs of $SO_2$, homo and lumo, are also shown in Fig. 2. The homo is symmetric and the lumo is antisymmetric as to the plane *m*. Now, the HOMO → lumo and homo → LUMO charge transfers (CT, and back CT) are *in phase* (symmetry-favorable). Concerted formation of two S–C bonds was expected.

The two CT interactions also work for the bond interchanges in the diene fragments. HOMO of **4** has bonding property on two olefinic bond (π bond) regions (C1–C2 and C4–C5), and antibonding property on the C2–C4 region. The electron-density loss from HOMO by the (HOMO → lumo) CT contributes to the cleavage of the C1–C2 and C4–C5 π bonds and the weakening of the antibonding character on the C2–C4 region. LUMO of **4** has antibonding property on two olefinic bond regions (C1–C2 and C4–C5) and bonding property on the C2–C4 region. The electron-density acceptance in LUMO via the (homo → LUMO) back CT contributes

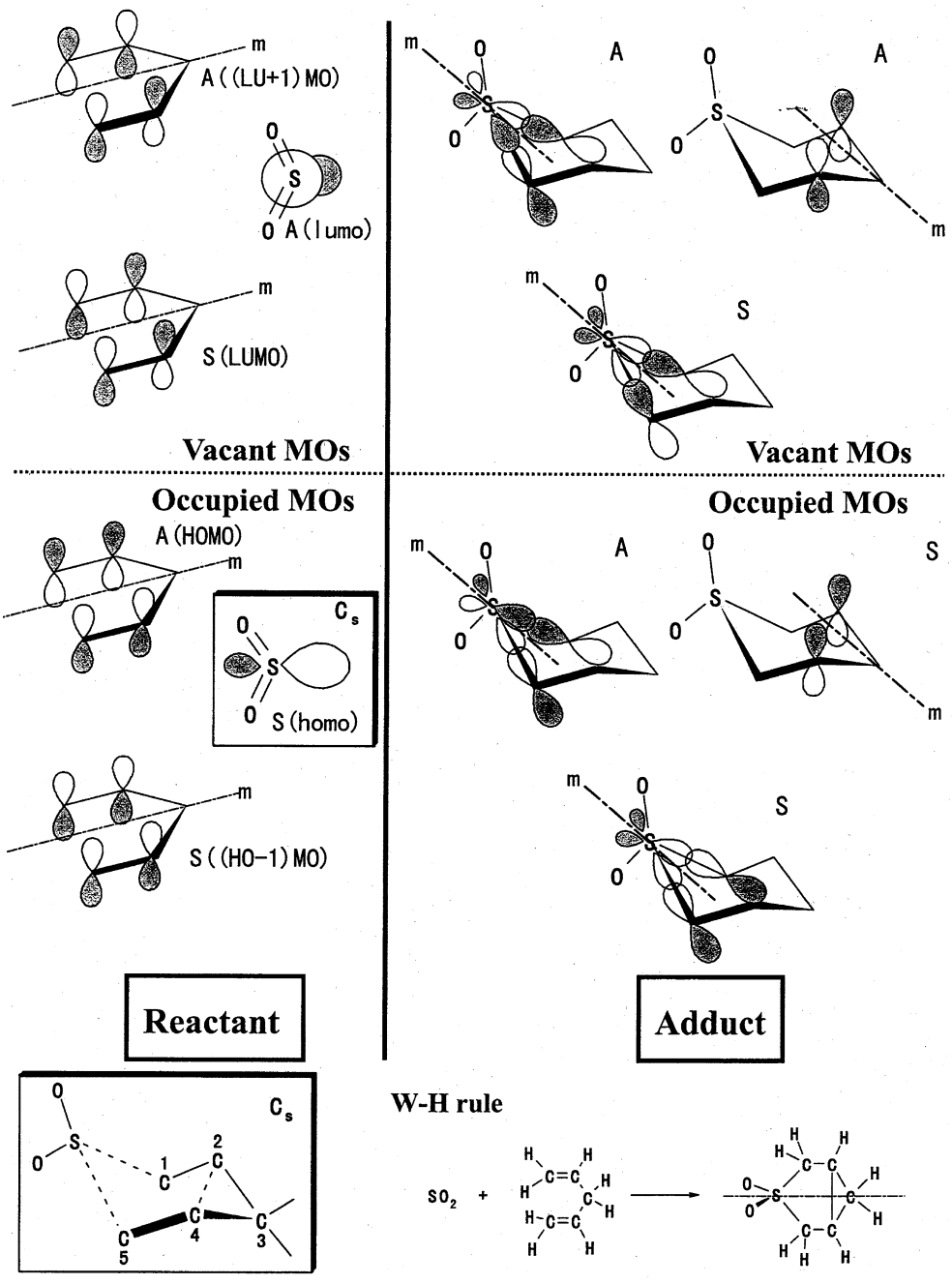


**Fig. 1.** An orbital correlation diagram of the Woodward-Hoffmann (*W–H*) rule along the $C_s$-symmetry conserving cheletropic addition. The reactants are 1,4-pentadiene (**4**) and $SO_2$. *Interrupted lines* show the $C_s$-symmetry mirror plane (*m*). *S* and *A* attached to all molecular orbitals (*MOs*) denote symmetric and antisymmetric orbitals, respectively, with respect to the mirror plane.

to the cleavage of two (C1–C2 and C4–C5) $\pi$ bonds and the formation of the C2–C4 bond, cyclopropane-ring formation. The CT and back CT operate reasonably to cause the reaction in Eq. (5). Both the CT and the back CT contribute to the formation of two S–C bonds ($O_2S\cdots C1$ and $O_2S\cdots C5$) and the cleavage of two olefinic bonds (C1 = C2 and C4 = C5), that is, change of double bonds to single bonds. The C2–C4 cyclopropane-ring formation is brought about both by the weakening of the antibonding nature of HOMO via the (HOMO $\rightarrow$ lumo) CT and by the appearance of the bonding nature of LUMO via the (homo $\rightarrow$ LUMO) back CT. Thus, the concerted and $C_s$-symmetry conserving mechanism of cheletropic additions forming cyclopropanes may be predicted by the FMO theory.

According to the normal electron demand for Diels–Alder (DA) reactions [7], CT works more than back CT to promote the reaction. There is a significant difference of CTs between the present and DA reactions (Scheme 2).

In the DA reaction, two C–C covalent bonds may be formed readily, because $2p\pi$ orbitals are aligned through the $sp^2 \rightarrow sp^3$ rehybridization. The $C_s$ symmetry may be conserved to complete the two C–C $\sigma$ bonds. On the

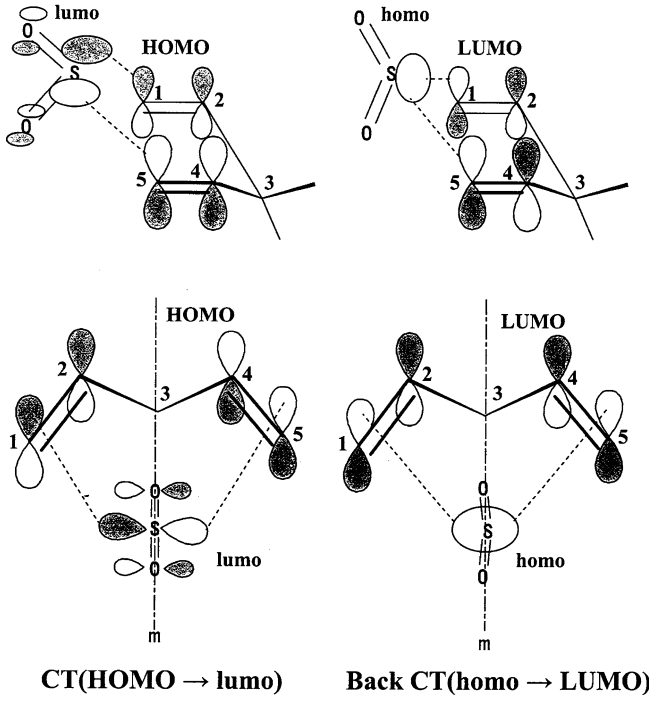


**Fig. 2.** Frontier MO (*FMO*) interactions between **4** and $SO_2$. *Interrupted lines* denote the $C_s$ mirror plane (*m*)

other hand, the $2p\pi$(C)–$3p\pi$(S) alignment is infeasible as far as the $C_s$ symmetry is imposed on the reaction path. The $C_s$-symmetry constraint precludes the $sp^2 \rightarrow sp^3$ rehybridization on the center of the reagent *X*, because the $p\pi$ orbital (antisymmetric) cannot mix with the *s* orbital (symmetric). If a large antisymmetric orbital overlap cannot be obtained in CT, the $C_s$-symmetry constraint should be relaxed. Once the relaxation is introduced, the $p\pi$–*s* mixing and the subsequent rehybridization are feasible to stabilize the reacting system. In this case, the W–H rule is violated, and CT and back CT operate in different regions (Fig. 3). It is necessary to examine numerically whether symmetry (in Fig. 2) or asymmetry (in Fig. 3) reaction paths are likely. The geometric conditions are taken into account by the parent and flexibly distortable diene (**4**) and the fixed-geometry diene (**5**). The size of the cheletropic reagents (*X*s) might affect the symmetry or asymmetry.

## 3 Method of calculation

For the ten addition paths given by the combination of 1,4-dienes and *X*s in Scheme 1, geometries of reactants (1,4-diene and *X*), addition transition states (TSs) and adducts were fully optimized using the B3LYP/6-31G*

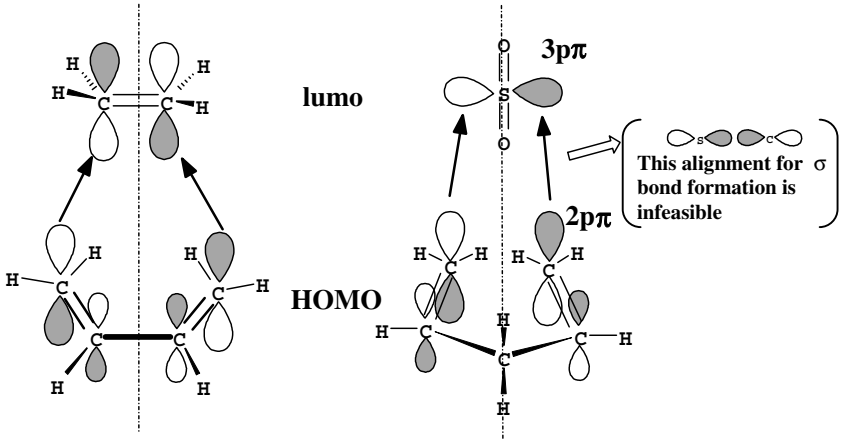


**Scheme 2.** Charge transfer (*CT*) interactions to form C–C and C–S covalent bonds.

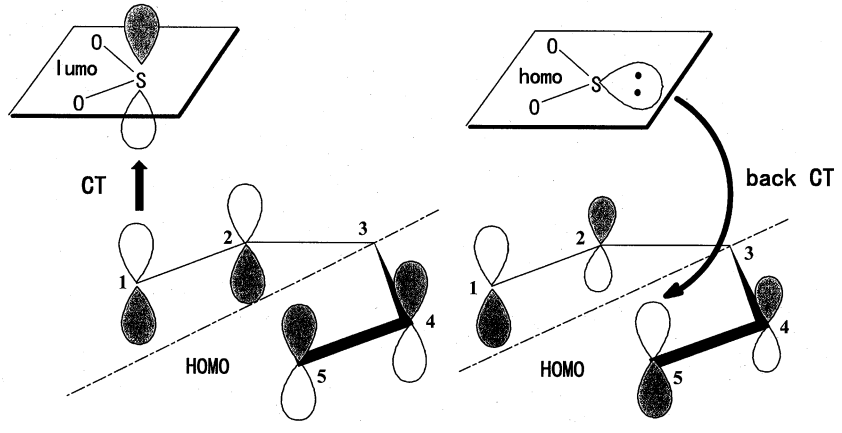


**Fig. 3.** FMO interactions in the donor–acceptor relationship without the $C_s$ symmetry.

method [8]. Subsequent vibrational analyses were carried out to check whether the TS geometries obtained are correct at the saddle points. Reaction paths were traced by means of the intrinsic reaction coordinate (IRC) [9] to check whether the reactions are concerted or stepwise.

The dependence of computational methods on the TSs of the additions of cheletropic reagents, *X* (*X* is CO, $SO_2$ and $EtPCl_2$), to 1,4-pentadiene (**4**) was examined. The TS structures were calculated by the restricted Hartree–Fock (RHF) method with the 6-31G* basis set (RHF/6-31G*), and by density-functional methods, B3LYP/6-31G*, B3LYP/6-311+G(2d,p), B3LYP/cc-pVTZ [10], BLYP/6-31G*, BLYP/6-311+G(2d,p), and BLPY/cc-pVTZ.

Configuration (quantitative fragment MO) analyses (CA) [11] were carried out at the TSs to evaluate numerically the orbital interactions. The MOs for CA were calculated using the RHF/STO-3G method on the optimized geometries using the B3LYP/6-31G* method.

All the calculations were performed using the GAUSSIAN 98 program package [12] installed on the Compaq ES40 computers of the Information Center of Nara University of Education and of the Computer Center of Nara University.

## 4 Calculated results and discussion

Figure 4 shows TS geometries of two cheletropic additions, **4**+CO and **5**+CO. They were found to have concerted characters, cheletropic formation of two covalent bonds, alternations of C1=C2 and C4=C5 double bonds to single bonds and C2–C4 bond formation (cyclopropanation). The TS structure of (**4**+CO) is similar to that of (**5**+CO). Clearly, the diene **4** is reactive, because it is free from the ring strain in the reactant and can accommodate the cheletropic addition. In this respect, it is noteworthy that the tricyclic diene **5** gives TS structures similar to those of **4**. The cyclohexyl ring supporting the diene moiety does not hinder the addition but makes the C2–C4 distance short (2.514 Å in **4** versus 2.382 Å in **5**) for the ready cyclopropanation. In Figs. 1 and 2, the $C_s$-symmetry conserving path was predicted. The symmetry is certainly conserved in Fig. 4.

Figure 5 shows two TS geometries for **4**+$SO_2$ and **5**+$SO_2$. While the former TS has $C_s$ symmetry, the latter does not (small violation of the W–H rule). While the linear diene **4** can make two S–C bonds (S–C1 and S–C5) flexibly, the fixed diene **5** cannot. A slight donor–acceptor role is involved in the latter TS. Figure 6 shows two TS geometries for **4**+$C_2H_5PCl_2$ and **5**+$C_2H_5PCl_2$. The same trend is seen in Figs. 5 and 6; the W–H rule holds or almost holds for the cheletropic additions.

In Figs. 7 and 8, the cheletropic reagents are divalent and more electrophilic than CO, $SO_2$ and $EtPCl_2$. The donor–acceptor relation is strengthened, and the TS geometries are very asymmetric (large violation of the W–H rule) according to the CT and back CT interactions in Fig. 3. The in-phase CT and back CT interactions in Fig. 2 may be applicable only to reacting systems having those interactions of similar magnitudes.

On the left side of Fig. 9, reaction-coordinate vectors of (1,4-dienes+$EtPCl_2$) are exhibited. Concerted

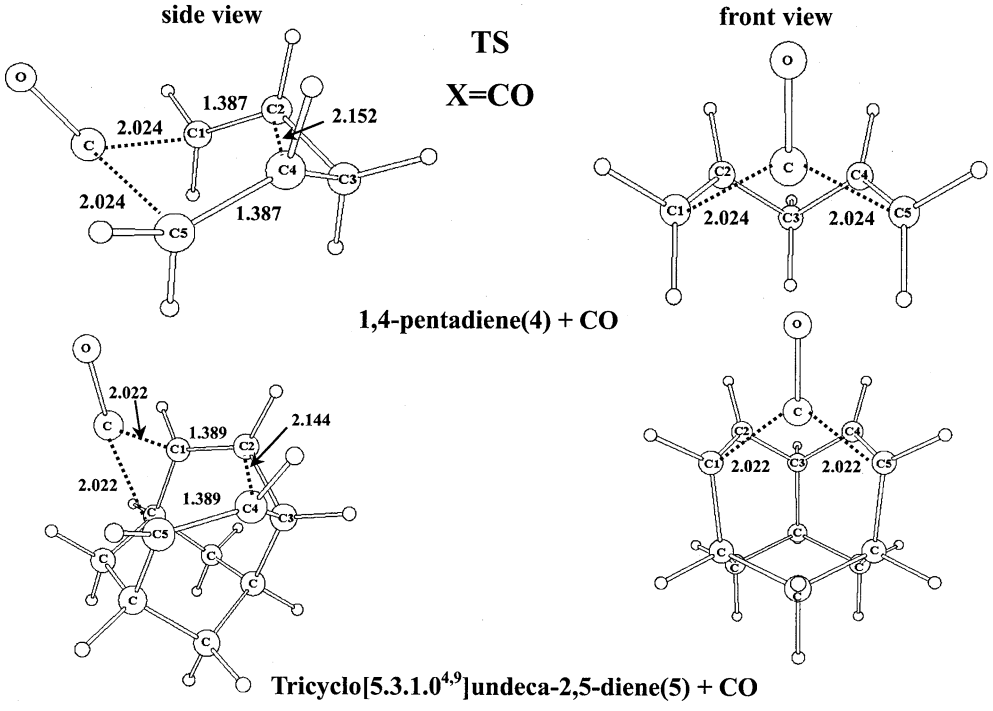


**Fig. 4.** Two transition-state (*TS*) geometries of cheletropic additions forming inside cyclopropane rings (Eq. 5). The cheletropic reagent *X* is carbon monoxide. *Empty circles* denote hydrogen atoms. Distances are in angstroms. Relative energies and sole imaginary frequencies are shown in Table 1.

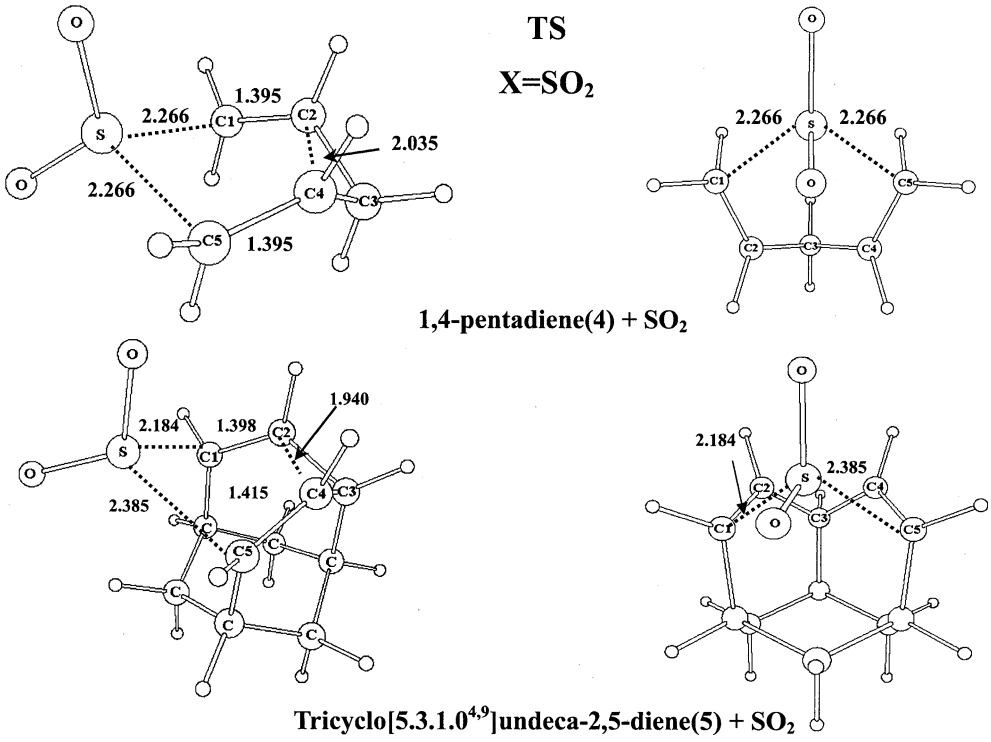


**Fig. 5.** Two TS geometries where *X* is sulfur dioxide.

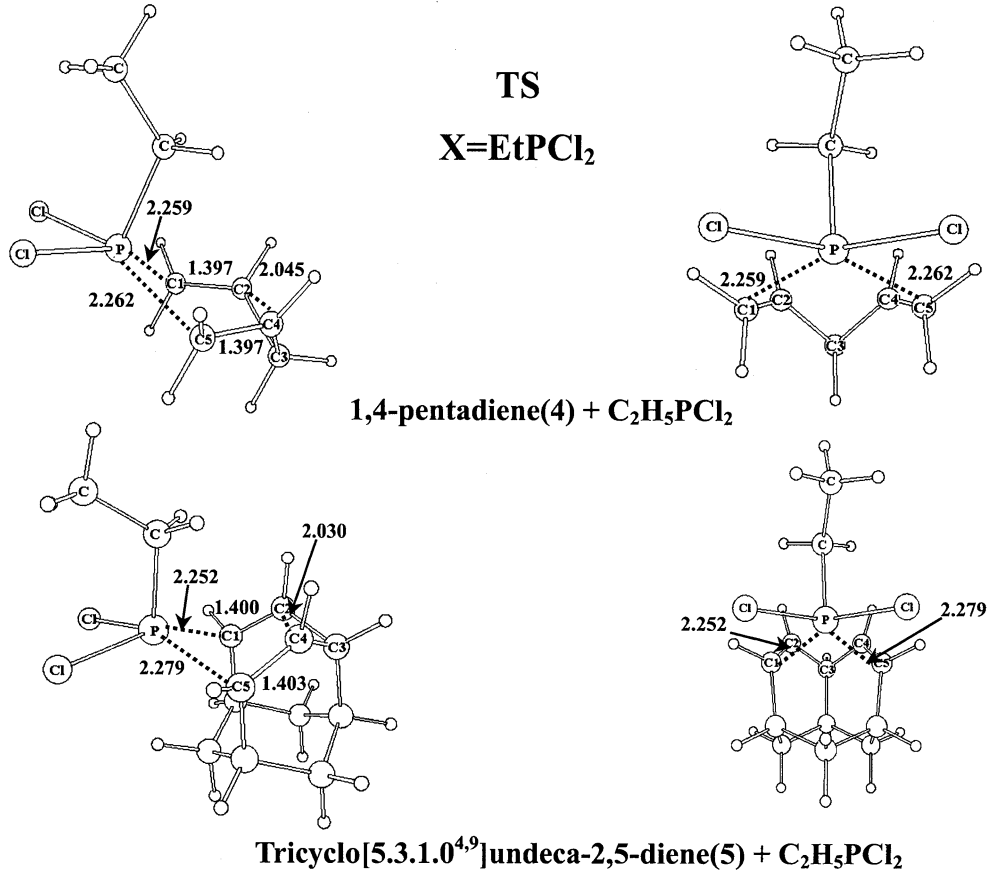


**Fig. 6.** Two TS geometries where *X* is dichloroethylphosphine.

motions are clearly shown. On the right side of Fig. 9, low-frequency symmetric vibrational modes of two 1,4-dienes are sketched. These modes correspond to those of the reaction-coordinate vectors of TSs. The vectors of $\nu_1$ of **4** and $\nu_2$ of **5** are fit both for the cheletropic addition and for the cyclopropane-ring closure. The P···C

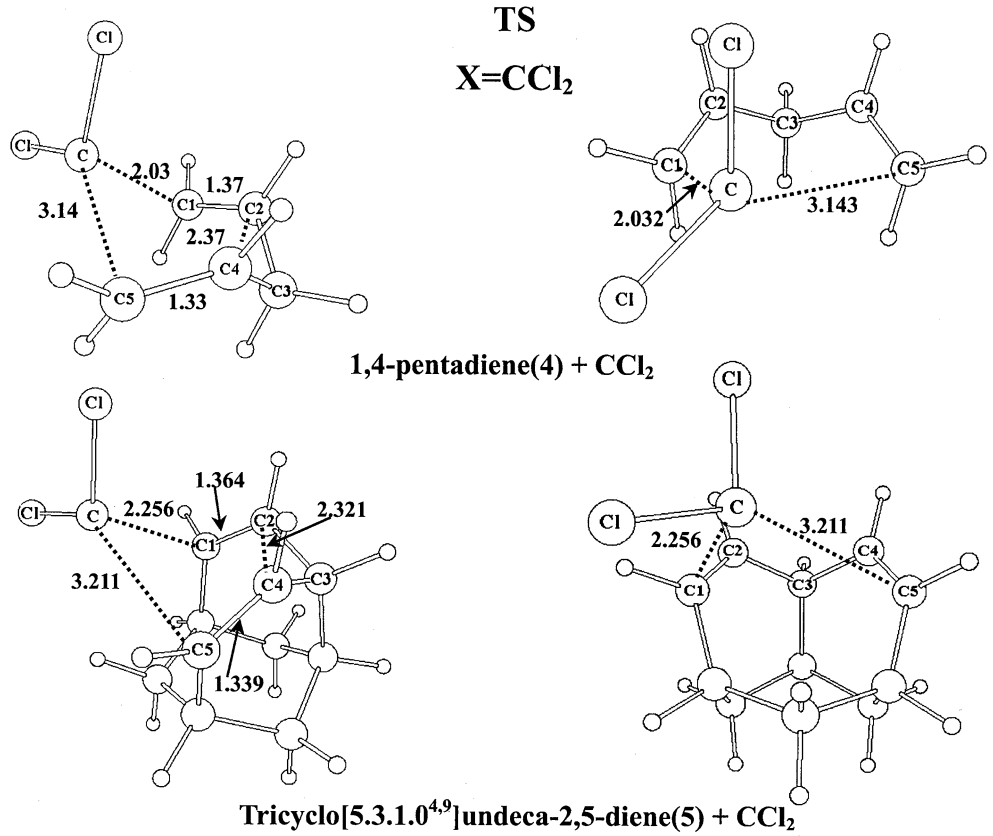


**Fig. 7.** Two TS geometries with $X$ is dichlorocarbene.

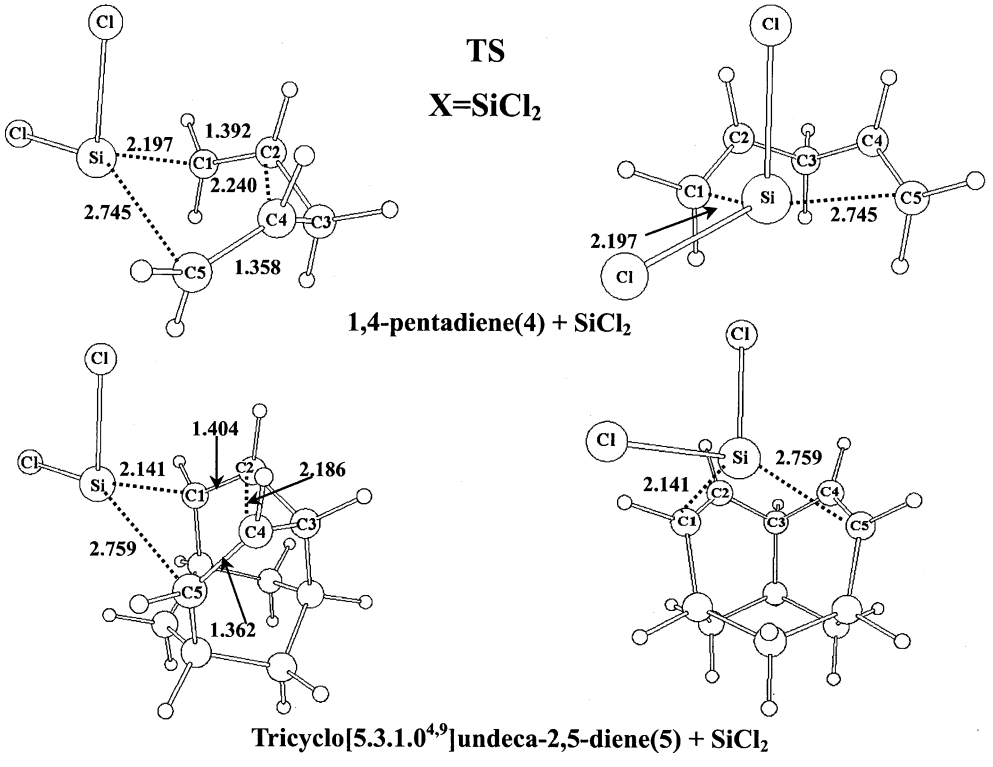


**Fig. 8.** Two TS geometries with $X$ is dichlorosilane.

approaching vector component deviates somewhat from the $C_s$ mirror plane, which indicates the slight donor–acceptor interaction of Fig. 3.

Table 1 shows activation energies of the ten reactions and sole imaginary frequencies. $X = CCl_2$ and $X = SiCl_2$ react with the two dienes with small activation energies,

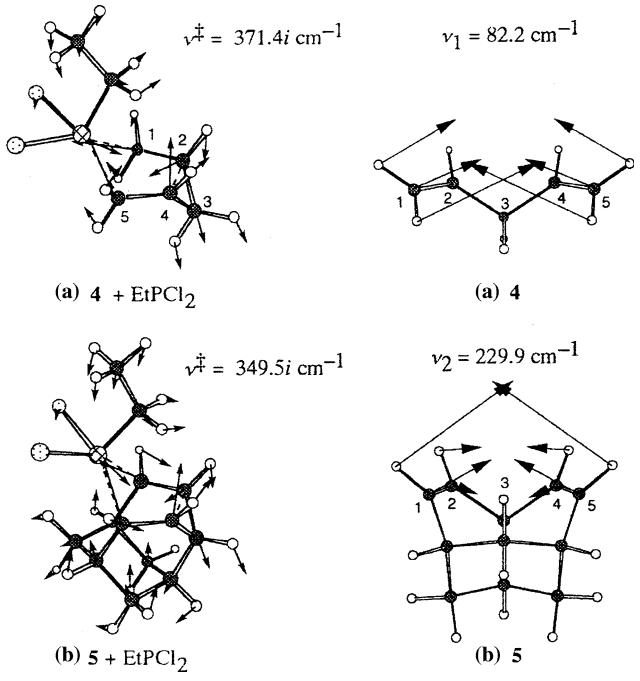


**Fig. 9.** *Left*, reaction-coordinate vectors at TSs corresponding to the sole imaginary frequency, $v^{\ddagger}$, for two reactions, (**a**) **4** + $EtPCl_2$ and (**b**) **5** + $EtPCl_2$. *Right*, low-frequency vibrational modes of dienes, (**a**) **4** and (**b**) **5**.

**Table 1.** Relative energies ($\Delta E$s) of transition states (*TS*s) calculated using B3LYP/6-31G* and sole imaginary frequencies $v^{\ddagger}$

| 1,4-Diene | Reagent *X* | $\Delta E$ (kJ mol$^{-1}$)[a] | $v^{\ddagger}$ (cm$^{-1}$) |
|---|---|---|---|
| 1,4-Pentadiene(**4**) | CO | 112.93 (117.07) | 486.1*i* |
| | $SO_2$ | 85.98 (95.14) | 394.0*i* |
| | $EtPCl_2$ | 104.68 (113.85) | 371.4*i* |
| | $CCl_2$ | 21.00 (22.47) | 267.0*i* |
| | $SiCl_2$ | 5.15 (25.69) | 187.4*i* |
| Tricyclo[5.3.1.0$^{4,9}$] undeca-2,5-diene(**5**) | CO | 95.06 (100.08) | 462.0*i* |
| | $SO_2$ | 71.25 (86.40) | 390.9*i* |
| | $EtPCl_2$ | 93.47 (100.21) | 349.5*i* |
| | $CCl_2$ | 4.90 (8.79) | 136.6*i* |
| | $SiCl_2$ | −2.97 (16.02) | 187.4*i* |

[a]There is a reactant like complex (aprecursor), **4**···X or **5**···X, andthe values in *parentheses* are differences of the total energies between precursors and TSs. Those without parentheses are differences between reactants and TSs

and *X* = CO and *X* = $EtPCl_2$ do so with similar and large activation energies. The cyclohexyl ring attached to the lower side of the 1,4-pentadiene moiety enhances the reactivity of **5**.

Table 2 exhibits TS geometries, activation energies and imaginary frequencies of the (**4** + *X*) reactions calculated by various methods. Generally, geometries are rather insensitive to the methods. RHF/6-31G* activation energies are unreasonably large. The difference

**Table 2.** Dependence of computational methods on various values of TSs in additions between 1,4-pentadiene and cheletropic reagents (*X* is CO, $SO_2$ and $EtPCl_2$). Distances and angles we defined in the following figure: 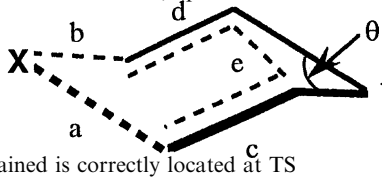

. $E_a$ is the activation energy. $v^{\ddagger}$ is the sole imaginary frequency which verifies that the geometry obtained is correctly located at TS

| (2–1)1,4-pentadiene + CO | | | | | | |
|---|---|---|---|---|---|---|
| | *a* (=*b*) (Å) | *c* (=*d*) (Å) | *e* (Å) | *θ*(°) | $E_a$ (kJ mol$^{-1}$) | $v^{\ddagger}$ (cm$^{-1}$) |
| RHF/6-31G* | 1.968 | 1.385 | 2.040 | 86.5 | 263.6 | 854.5*i* |
| B3LYP/6-31G* | 2.024 | 1.387 | 2.152 | 91.7 | 113.0 | 486.2*i* |
| B3LYP/6-311+ G (2d,p) | 2.001 | 1.384 | 2.134 | 91.1 | 137.2 | 505.7*i* |
| B3LYP/cc-pVTZ | 1.999 | 1.384 | 2.125 | 90.7 | 137.7 | 507.5*i* |
| BLYP/6-31G* | 2.039 | 1.398 | 2.197 | 93.3 | 93.3 | 410.4*i* |
| BLYP/6-311 + G(2d,p) | 2.009 | 1.396 | 2.176 | 92.4 | 120.1 | 432.5*i* |
| BLYP/cc-pVTZ | 2.005 | 1.395 | 2.165 | 92.0 | 120.5 | 433.5*i* |
| (2–2)1,4-pentadiene + $SO_2$ | | | | | | |
| | *a* (=*b*) (Å) | *c* (=*d*) (Å) | *e* (Å) | *θ*(°) | $E_a$ (kJ mol$^{-1}$) | $v^{\ddagger}$ (cm$^{-1}$) |
| RHF/6-31G* | 2.261 | 1.382 | 2.010 | 85.1 | 193.3 | 682.6*i*[a] |
| B3LYP/6-31G* | 2.266 | 1.395 | 2.035 | 85.9 | 86.2 | 394.0*i* |
| B3LYP/6-311 + G(2d,p) | 2.248 | 1.393 | 2.013 | 85.0 | 103.3 | 404.5*i* |
| B3LYP/cc-pVTZ | 2.250 | 1.392 | 2.007 | 84.8 | 103.3 | 407.8*i* |
| BLYP/6-31G* | 2.233 | 1.417 | 2.001 | 83.5 | 84.2 | 347.8*i* |
| BLYP/6-311 + G(2d,p) | 2.216 | 1.415 | 1.970 | 82.8 | 102.1 | 361.4*i* |
| BLYP/cc-pVTZ | 2.218 | 1.414 | 1.963 | 81.9 | 102.1 | 365.6*i* |
| (2–3)1,4-pentadiene + $EtPCl_2$ | | | | | | |
| | *a* (=*b*) (Å) | *c* (=d) (Å) | *e* (Å) | *θ*(°) | $E_a$ (kJ mol$^{-1}$) | $v^{\ddagger}$ (cm$^{-1}$) |
| RHF/6-31G* | 2.263 (2.265) | 1.389 (1.389) | 1.972 | 83.3 | 232.6 | 670.2*i* |
| B3LYP/6-31G* | 2.259 (2.262) | 1.397 (1.397) | 2.045 | 86.5 | 104.6 | 371.4*i* |
| B3LYP/6-311 + G(2d,p) | 2.243 (2.246) | 1.393 (1.392) | 2.037 | 86.3 | 121.8 | 375.3*i* |
| B3LYP/cc-pVTZ | 2.243 (2.246) | 1.393 (1.392) | 2.023 | 85.6 | 126.8 | 384.5*i* |
| BLYP/6-31G* | 2.234 (2.235) | 1.415 (1.415) | 2.049 | 85.9 | 96.7 | 306.9*i* |
| BLYP/6-311 + G(2d,p) | 2.223 (2.225) | 1.409 (1.409) | 2.038 | 85.6 | 117.6 | 313.8*i* |
| BLYP/cc-pVTZ | 2.218 (2.219) | 1.411 (1.410) | 2.017 | 84.6 | 122.2 | 325.0*i* |

[a]Another imaginary frequency, 10.9*i* cm$^{-1}$, is obtained with $C_S$ symmetry

between those of other methods are 19–33 kJ/mol and are somewhat dependent on the methods. Overall, the B3LYP/6-31G* method used in Figs. 4, 5, 6, 7 and 8 and in Table 1 would be of tolerable accuracy.

Computational results are summarized. 1,4-Dienes (**4** and **5**) react with cheletropic reagents (CO, $SO_2$, $EtPCl_2$, $CCl_2$ and $SiCl_2$) concertedly affording cyclopropane moieties according to IRC calculations. As a whole, reactant **4** gives $C_s$-symmetry or nearly $C_s$-symmetry reaction paths, while reactant **5** gives $C_1$-symmetry ones. The larger the donor–acceptor interaction becomes, the larger the deviation is.

## 5 Results of configuration analyses and discussions

In Figs. 2 and 3, orbital-interaction schemes are presented. The reactivities of two dienes (**4** and **5**) are compared. The cyclohexyl group supporting the 1,4-pentadiene moiety makes **5** more electron-donating. The HOMO level (–0.263 au by RHF/STO-3G) of **5** is much higher than that (–0.307 au) of its parent 1,4-diene, **4**. The LUMO level (0.292 au) of **5** is also lower than that (0.304 au) of **4**. These energy-level differences are caused by the cyclohexyl group. The HOMO of 1,4-diene is composed of two olefinic $\pi$ bonds ($\pi$1 and $\pi$2 in Scheme 3). The energy level of the HOMO depends upon the interaction between $\pi$1 and $\pi$2. The cyclohexyl group makes the two olefinic bonds come closer to each other. Then, the $\pi$1–$\pi$2 interaction in **5** becomes large as a first approximation. Consequently, the HOMO level of **5** is higher than that of **4**. A similar discussion holds for the LUMO levels (Scheme 3).

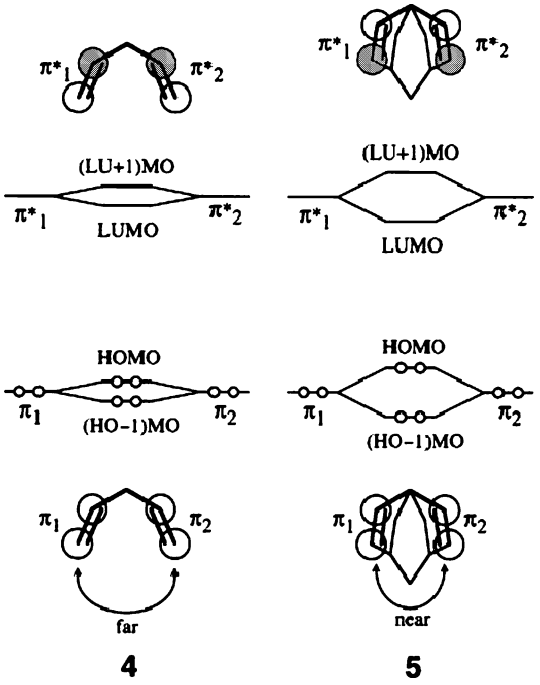


**Scheme 3.** The first mixing of two olefinic $\pi$ (or $\pi^*$) orbitals.

In order to examine orbital interactions quantitatively, CA [11] was carried out and the results are shown in Table 3. Absolute values of the coefficients of the main electron configurations are displayed. The coefficient $C_0$ shows the extent of reactant (**4** + *X*) electron configurations (the zeroth order). Except for $C_0$, the (HOMO → lumo) CT interaction contributes most to the reaction progress. This result is consistent both with the prediction in Figs. 2 and 3 and with the normal electron demand [7]. The (homo → LUMO) back CT follows generally CT. The prediction made in Figs. 2 and 3 has been confirmed. The extent of the difference between (HOMO → lumo) and (homo → LUMO) may be related to that of the asymmetry of the TS structures. These of (**4** + CO), (**4** + $SO_2$) and (**4** + $EtPCl_2$) are symmetric or nearly symmetric according to the in-phase FMO interaction in Fig. 2. Those of (**4** + $CCl_2$) and (**4** + $SiCl_2$) are asymmetric according to the donor–acceptor FMO interaction in Fig. 3. The coefficient values in Table 3 show (HOMO → lumo)≅(homo → LUMO) for the in-phase FMO and (HOMO → lumo) > (homo → LUMO) for the donor–acceptor FMO. For **4** + $CCl_2$, CA values at the $C_s$-symmetry constrained TS (not a real TS) geometry were obtained and are shown in parentheses. As expected, the donor–acceptor relation is weakened by the constraint.

The unexpectedly large contribution of the polarization (one-electron excitation electron configuration), (HO−1)MO → LUMO in **4** + CO and **4** + $EtPCl_2$, is noteworthy. Both MOs are symmetric with respect to the mirror plane (*m* in Fig. 1 and the interrupted lines in Fig. 2), and the excitation works effectively to elongate C1–C2 and C4–C5 bonds in response to the antibonding character of LUMO. More importantly, the mixing-in of (HO−1)MO to LUMO enlarges the lobes for the cyclopropanation (the lobes of C2 and C4). When *X* approaches the 1,4-diene, homo (*X*) interacts with (HO−1)MO and LUMO. The mixing of (HO−1)MO and LUMO is the largest in "new homo" in Scheme 4. In new homo, (HO−1)MO and LUMO intermix with each other in the opposite sign through the overlap with homo. This orbital mixing enlarges the lobes of the carbon atoms (C2 and C4) for the cyclopropanation (Scheme 4).

The large contribution of the polarization, (HO−1)MO → LUMO, is also observed in the typical DA reaction between butadiene and ethylene. The result of the configuration analysis at the TS is $C_0 = 0.747$, HOMO → lumo = 0.278, homo → LUMO = 0.272 and (HO−1)MO → LUMO = 0.085. The polarization caused by the orbital mixing helps the intramolecular bond formation generally.

## 6 Symmetry or asymmetry in cheletropic additions.

In Sect. 2, the addition path for 1,4-pentadiene (**4**) and $SO_2$ was examined by the W–H rule and FMO theory. The W–H rule predicted that the path should conserve

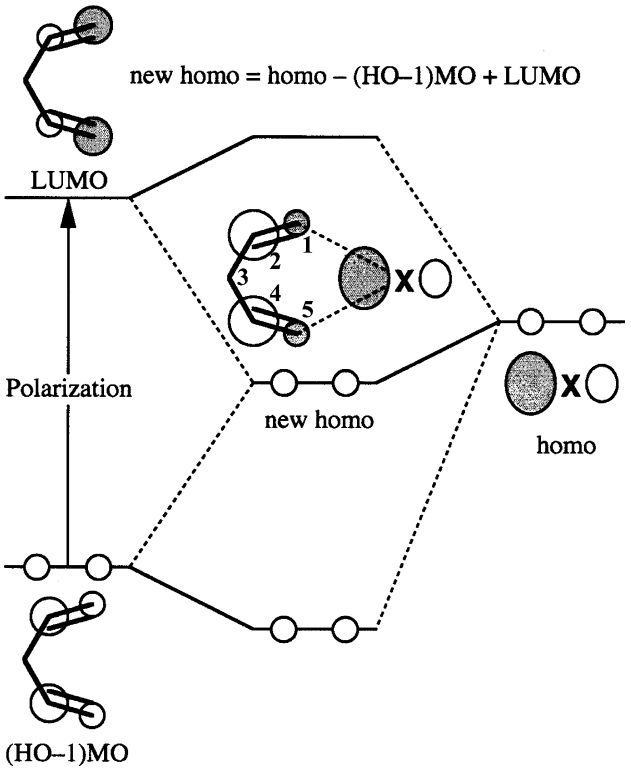


**Scheme 4.** Three-orbital mixing, new homo = homo−(HO−1)-MO + LUMO, to enlarge the lobes of C2 and C4.

the $C_s$ symmetry. The FMO theory predicted either the $C_s$-symmetry path based on the in-phase FMO overlap or the $C_1$-symmetry one on the donor–acceptor interaction. The computational results of TS geometries (Figs. 4, 5, 6, 7, 8) have shown there are $C_s$- and $C_1$-symmetry paths. Both (**4** + CO) and (**5** + CO) have $C_s$ symmetry (Fig. 4). A large back CT (homo → LUMO = 0.234 in Table 3) controls the symmetry irrespective of the reactant dienes (**4** or **5**). Orbitals ($\pi_1$* and $\pi_2$*) are used to promote CT (the right half of Scheme 5).

The orthogonality is confirmed in the $C_1 \cdots CO \cdots C_2$ angles, 97.4° and 92.3°, of the (**4** + CO) TS and the (**5** + CO) TS (Fig. 4), respectively. Except for three reactions, (**4** + CO), (**5** + CO) and (**4** + $SO_2$), the reactions have $C_1$-symmetry paths. The deviation from the $C_s$-symmetry plane is larger for $X = CCl_2$ than for $X = SiCl_2$. The C–C bond formation requires severer bond directionality than the Si–C one, because the carbon atom is harder than the silicon one [13]. The more inflexible substrate **5** gives asymmetry compared with **4**. Thus, the present cheletropic additions generally take the $C_1$-symmetry paths and do not follow the W–H rule. They are critical between the in-phase FMO overlap (with $C_s$ symmetry, Fig. 2) and the donor–acceptor interaction (without $C_s$ symmetry, Fig. 3). The donor–acceptor interaction is enhanced, when the (lumo–HOMO) energy gap is smaller than the (LUMO–homo) one. In Fig. 10, correlations between the energy-gap ratio, ratio($E$), and the extent of asymmetry of TS geometries, ratio($l$), are shown. As ratio($E$) becomes large, ratio($I$) deviates from 1.000. The critical value, ratio($E$) = 1.4, may be defined arbitrarily. Thus, ratio($E$) is a criterion to distinguish symmetric TS geometries from asymmetric ones.

A similar contrast was reported in cheletropic reactions between butadiene (**1**) and $SO_2$ uncatalyzed or

**Table 3.** Results of the configuration analyses on theTSs of the cheletropic additions between 1,4-pentadiene and $X$ ($X$ is CO, $SO_2$, $EtPCl_2$, $CCl_2$ and $SiCl_2$). $C_0$ is the coefficient for the adiabatic-interaction configuration (without any electron transfer or excitation). The coefficients (absolute value) of more than 0.1 are taken up. HOMO, (HO−1)MO, LUMO, (LU + 1)MO, homo and lumo are shown at the reactant side in Fig. 1. The values in *parentheses* are for the $C_s$-symmetry contrained TS geometry

| | | |
|---|---|---|
| 1,4-Pentadiene + CO | | |
| $C_0$ | 0.625 | Adiabatic |
| HOMO → lumo | 0.254 | Charge transfer |
| homo → LUMO | 0.234 | Backcharge transfer |
| (HO−1)MO → LUMO | 0.129 | Polarization |
| 1,4-Pentadiene + $SO_2$ | | |
| $C_0$ | 0.687 | Adiabatic |
| HOMO → lumo | 0.298 | Charge transfer |
| homo → LUMO | 0.240 | Back charge transfer |
| (HO−1)MO → LUMO | 0.102 | Polarization |
| 1,4-Pentadiene + $EtPCl_2$ | | |
| $C_0$ | 0.603 | Adiabatic |
| HOMO → lumo | 0.272 | Charge transfer |
| homo → LUMO | 0.230 | Back charge transfer |
| HOMO → (LU + 1)MO | 0.104 | Polarization |
| (HO−1)MO → LUMO | 0.104 | Polarization |
| 1,4-Pentadiene + $CCl_2$ | | |
| $C_0$ | 0.759 (0.881) | Adiabatic |
| HOMO → lumo | 0.302 (0.254) | Charge transfer |
| (HO-1)MO → lumo | 0.146 (0.040) | Charge transfer |
| homo → LUMO | 0.105 (0.118) | Back charge transfer |
| homo → lumo | 0.125 (0.0) | Polarization |
| 1,4-Pentadiene + $SiCl_2$ | | |
| $C_0$ | 0.678 | Adiabatic |
| HOMO → lumo | 0.264 | Charge transfer |
| homo → LUMO | 0.183 | Back charge transfer |
| (HO−1)MO → lumo | 0.130 | Charge transfer |

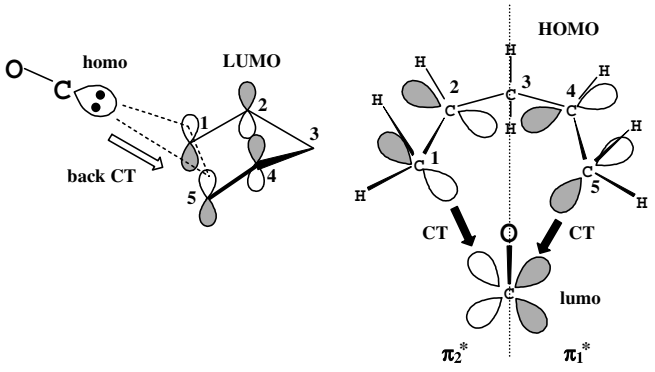


**Scheme 5.** Frontier molecular orbital interactions to support the $C_s$-symmetry addition path.

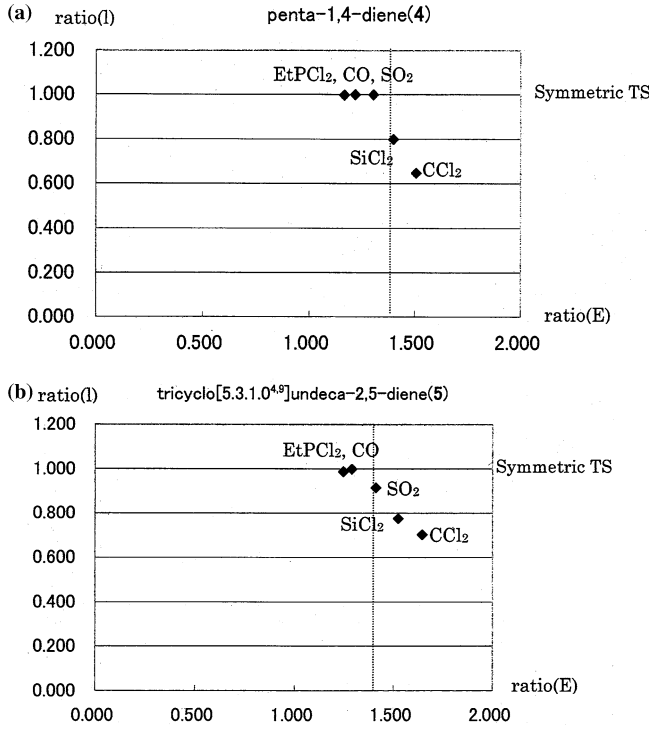


**Fig. 10.** Correlations between the donor–acceptor strength and the asymmetry of the obtained TS geometries. For the abscissa, ratio($E$) means the ratio of the gaps of the frontier orbital energies, (LUMO–homo)/(lumo–HOMO). HOMO and LUMO belong to the diene (**4** and **5**) and homo and lumo to the reagent $X$ as shown in Fig. 2. The larger value of ratio($E$) corresponds to the stronger donor–acceptor relation. For the ordinate, ratio($l$) means the ratio of two $X\cdots$C distances ($X\cdots$C1 and $X\cdots$C5) in the TS geometries of Figs. 4, 5, 6, 7 and 8. Ratio($l$) < 1.00 corresponds to the more asymmetric TS structure. Ratio($E$) = 1.40 (the *vertical dotted line*) may be a borderline between symmetric [ratio($l$) = 1.000] and asymmetric TS structures.

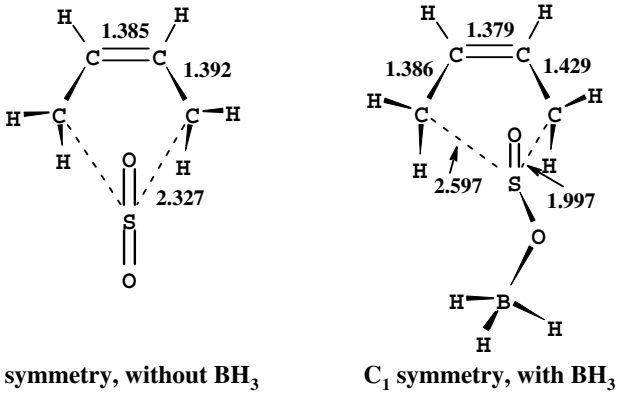


**$C_s$ symmetry, without $BH_3$** **$C_1$ symmetry, with $BH_3$**

**Scheme 6.** Transition-state geometries of different point groups for cheletropic additions between butadiene and $SO_2$ (without and with a Lewis acid, $BH_3$) [14].

catalyzed by $BH_3$ (Scheme 6) [14]. The reason for the contrast was not discussed in the literature [14]. According to the present classification, the $BH_3$-free reaction obeys the in-phase FMO interaction of Fig. 2

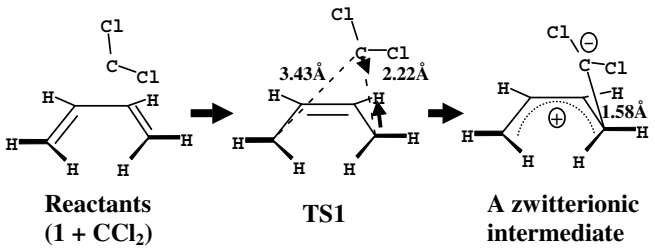


**Scheme 7.** A one-center (not cheletropic) addition between butadiene and dichlorocarbene.

and the $BH_3$-containing one follows the donor–acceptor one of Fig. 3. Our calculation on a model system, butadiene and $CCl_2$, was also made and the system takes the $C_1$-symmetry addition path. The large asymmetry leads to not a concerted but to a stepwise path (Scheme 7) as an extreme case. The stepwise path of (**1** + $CCl_2$) is in contrast with the concerted path of **4** + $CCl_2$ (Fig. 7). The conjugated diene **1** has rigid planarity and cannot conform to simultaneous formation of two C–C ($Cl_2C$–C1 and $Cl_2C$–C5) bonds via $sp^2 \rightarrow sp^3$ rehybridization.

In our previous work, combinations of strong donor dienes and strong acceptor olefins were found to give asymmetric cycloaddition paths [15]. When the donor and/or the acceptor ability is weakened, normal $C_s$-symmetry paths were obtained. It is a matter of degree whether the symmetric or the asymmetric path is taken. Generally speaking, the DA reactions tend to take symmetric paths, and the cheletropic ones take asymmetric paths. A crucial difference between those reactions is in the degree of flexibility for $sp^2 \rightarrow sp^3$ rehybridization between the dienophile (olefin) and the cheletropic reagent $X$.

## 7 Concluding remarks

This work has dealt theoretically with ten cheletropic additions forming inside cyclopropane rings. They are all of concerted processes with synchronous or almost synchronous formation of $X$–C1, $X$–C5 and C2–C4 (cyclopropane-ring closure) bonds and alternation of C1 = C2 and C4 = C5 double bonds to single ones. The diene **5** is a suitable reactant to lower activation energies.

The most typical example of the FMO theory is the DA reaction [6]. The theory describes well bond formation and interchange. The present cheletropic additions forming a cyclopropane moiety would be as representative as DA reactions for the theory. A $\sigma$ (C2–C4) bond is formed at a site distant from the reaction center. Cyclopropane may be formed by the [homo–(HO−1)MO + LUMO] three-orbital mixing in the cheletropy additions.

Cheletropic additions between dienes and $X$s do not follow the W–H rule generally. Three-center interactions to form two $\sigma$ bonds simultaneously undergo steric strains and are not in line with the C–$X$ bond

directionality. There is a borderline between the in-phase FMO overlap (Fig. 2) and the donor–acceptor interaction (Fig. 3). When the reagent $X$ is a strong electrophile, the later interaction is favored and the reaction takes the $C_1$-symmetry path.

*Acknowledgments* This work was supported by a Grant-in-Aid for Scientific Research from the Ministry of Education, Science and Culture, Japan and by Nishida Memorial Foundation for Fundamental Chemical Research.

## References

1. Woodward RB, Hoffmann R (1970) The conservation of orbital symmetry. Verlag Chemie; New York, chap 10.1
2. Birney DM, Ham S, Unruh GR (1997) J Am Chem Soc 119:4509
3. Jung F, Molin M, Van Den Elzen R (1974) J Am Chem Soc 96:935
4. (a) Mocku WL (1970) J Am Chem Soc 92:6918; (b) Mock WL (1973) J Am Chem Soc 95:4472
5. Toda M, Miyahara I, Hirotsu K, Yamaguchi R, Kozima S, Matsumoto K (1991) Chem Lett 1677
6. Fukui K (1970) Theory of orientation and stereoselection. Springer, Berlin Heidelberg, New York
7. Sustmann R, Schubert R (1972) Angew Chem Int Ed Engl 11:840
8. Becke AD (1993) J Chem Phys 98:5648
9. (a) Fukui K (1970) J Phys Chem 74:4161; (b) Gonzalez C, Schlegel HB (1989) J Phys Chem 90:2154
10. (a) Woon DE, Dunning TH Jr (1993) J Chem Phys 98:1358; (b) Kendall RA, Dunning TH Jr, Harrison RJ (1992) J Chem Phys 96:6796
11. (a) Baba H, Suzuki S, Takemura T (1969) J Chem Phys 50:2078; (b) Fujimoto H, Kato S, Yamabe S, Fukui K (1974) J Chem Phys 60:572
12. Frisch MJ, Trucks GW, Schlegel HB, Scuseria GE, Robb MA, Cheeseman JR, Zakrzewski VG, Montgomery JA Jr, Stratmann RE, Burant JC, Dapprich S, Millam JM, Daniels AD, Kudin KN, Strain MC, Farkas O, Tomasi J, Barone V, Cossi M, Cammi R, Mennucci B, Pomelli C, Adamo C, Clifford S, Ochterski J, Petersson GA, Ayala PY, Cui Q, Morokuma K, Malick DK, Rabuck AD, Raghavachari K, Foresman JB, Cioslowski J, Ortiz JV, Baboul AG, Stefanov BB, Liu G, Liashenko A, Piskorz P, Komaromi I, Gomperts R, Martin RL, Fox DJ, Keith T, AI-Laham MA, Peng CY, Nanayakkara A, Gonzalez C, Challacombe M, Gill PMW, Johnson B, Chen W, Wong MW, Andres JL, Gonzalez C, Head-Gordon M, Replogle ES, Pople JA (1998) GAUSSIAN 98, revision A.7. Gaussian, Pittsburgh, PA
13. Pearson RG (1968) J Chem Educ 45:643
14. Suárez D, Sordo TL, Sordo JA (1995) J Org Chem 60:2848
15. Yamabe S, Nishihara Y, Minato T (2002) J Phys Chem A 106:4980